Inorg. Chem. **2003**, *42*, 6071–6080

Syntheses, Structures, and Properties of Imidazolate-Bridged Cu(II)–Cu(II) and Cu(II)–Zn(II) Dinuclear Complexes of a Single Macrocyclic Ligand with Two Hydroxyethyl Pendants

Dongfeng Li,* Shuan Li,* Dexi Yang, Jiuhong Yu, Jin Huang, Yizhi Li, and Wenxia Tang

State Key Laboratory of Coordination Chemistry, Coordination Chemistry Institute, Nanjing University, Nanjing 210093, P. R. China

Received March 29, 2003

The imidazolate-bridged homodinuclear Cu(II)–Cu(II) complex, $[(CuimCu)L]ClO_4 \cdot 0.5H_2O$ (**1**), and heterodinuclear Cu(II)–Zn(II) complex, $[(CuimZnL_{-2H})(CuimZnL_{-H})](ClO_4)_3$ (**2**), of a single macrocyclic ligand with two hydroxyethyl pendants, L (L = 3,6,9,16,19,22-hexaaza-6,19-bis(2-hydroxyethyl)tricyclo[22,2,2,$2^{11,14}$]triaconta-1,11,13,24,27,29-hexaene), have been synthesized as possible models for copper–zinc superoxide dismutase (Cu_2,Zn_2-SOD). Their crystal structures analyzed by X-ray diffraction methods have shown that the structures of the two complexes are markedly different. Complex **1** crystallizes in the orthorhombic system, containing an imidazolate-bridged dicopper(II) $[Cu–im–Cu]^{3+}$ core, in which the two copper(II) ions are pentacoordinated by virtue of an N4O environment with a Cu···Cu distance of 5.999(2) Å, adopting the geometry of distorted trigonal bipyramid and tetragonal pyramid, respectively. Complex **2** crystallizes in the triclinic system, containing two similar Cu–im–Zn cores in the asymmetric unit, in which both the Cu(II) and Zn(II) ions are pentacoordinated in a distorted trigonal bipyramid geometry, with the Cu···Zn distance of 5.950(1)/5.939(1) Å, respectively. Interestingly, the macrocyclic ligand with two arms possesses a chairlike (*anti*) conformation in complex **1**, but a boatlike (*syn*) conformation in complex **2**. Magnetic measurements and ESR spectroscopy of complex **1** have revealed the presence of an antiferromagnetic exchange interaction between the two Cu(II) ions. The ESR spectrum of the Cu(II)–Zn(II) heterodinuclear complex **2** displayed a typical signal for mononuclear trigonal bipyramidal Cu(II) complexes. From pH-dependent ESR and electronic spectroscopic studies, the imidazolate bridges in the two complexes have been found to be stable over broad pH ranges. The cyclic voltammograms of the two complexes have been investigated. Both of the two complexes can catalyze the dismutation of superoxide and show rather high activity.

Introduction

Superoxide dismutase (SOD) is one of the most crucial enzymes in the defense system of organisms for its ability to protect cells from the damage of the toxic superoxide, by catalyzing the dismutation of superoxide radicals effectively.[1] The X-ray crystal analysis[2] reveals that the active site of copper−zinc superoxide dismutase (Cu_2,Zn_2-SOD) from the bovine erythrocytes is composed of two identical subunits each containing a unique imidazolate-bridged bimetallic center with one copper(II) and one zinc(II) ion in its active site. A schematic view of its active site is shown in Scheme 1. The Cu^{2+} ion is coordinated by four histidines and a water ligand in a distorted square planar N4O coordination sphere, while the zinc ion is coordinated to an aspartate and three histidines, one of them bridging to copper. Studies on Cu_2,Zn_2-SOD have demonstrated that (i) the copper site, playing a direct role in the catalytic electron transfer mechanism, is cyclically reduced and oxidized by superoxide,

Scheme 1. Schematic View of Cu_2,Zn_2-SOD Active Site

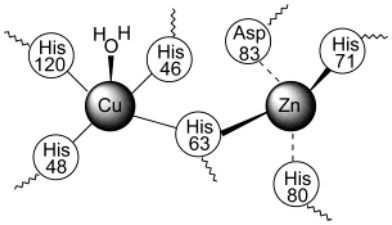

* Corresponding authors. E-mail: chem1121@nju.edu.cn (D.L.). Fax: +86-25-3314502 (D.L.); li_shuan@yahoo.com.cn (S.L.).

(1) Fridovich, I. *Annu. Rev. Biochem.* **1975**, *44*, 147.
(2) Tainer, J. A.; Getzoff, E. D.; Richardson, J. S.; Richardson, D. C. *Nature* **1983**, *306*, 284.

10.1021/ic034338g CCC: $25.00
Published on Web 08/23/2003

with the breakage and rejoining of the imidazole bridge; (ii) the catalytic rate constant and the spectroscopic properties are nearly pH-independent over the broad pH range 5.0−9.5.[3]

These striking features of Cu_2,Zn_2-SOD have attracted much attention in the past years. Many efforts have been devoted to the design and synthesis of Cu−Cu and Cu−Zn dinuclear complexes to mimic the spectroscopic, magnetic, and structural properties of the active site of Cu_2,Cu_2-SOD/Cu_2,Zn_2-SOD, following the pioneering work of Lippard's group.[4] Also, a number of imidazolate-bridged dicopper(II) complexes have been synthesized and characterized, and some of these models show good activities of dismutation of superoxide radical.[4−17] Compared with the imidazolate-bridged dicopper(II) complexes, however, structural characterized imidazolate-bridged heterodinuclear copper(II)−zinc(II) complexes are still very rare to date.[18]

In our previous work, we have utilized small molecule ligands (such as 4-diethylenetriamineacetate and triethylenetetramine) to achieve imidazolate-bridged heterodinuclear Cu(II)−Zn(II) complexes. However, the solution pH-dependent ESR studies show the imidazolate bridge in these Cu(II)−Zn(II) complexes to be stable only over a narrow range at high pH ca. 10 ∼ 12.[18d,e] To overcome such deficiency, Pierre et al.[18a] utilized a cryptand L′ (L′ = 1,4,12,15,18,26,31,39-octaazapentacyclo[13,13,13,1,^{6,10}1,^{20,24}1^{33,37}]-tetratetracontane-6,8,10,20,22,24,33,35,37-nonaene) to construct successfully an imidazolate-bridged Cu−Zn complex, [(CuimZn)L′]$(ClO_4)_3$, which has been found to be stable over a large pH range. Recently, Ohtsu et al.[18b] synthesized a unique dinucleating ligand Hbdpi containing an imidazole group [Hbdpi is 4,5-bis(di(2-pyridylmethyl)aminomethyl)-imidazole] and used it to obtain a heterodinuclear Cu−Zn complex bridged by the imidazolate group of the ligand.

Scheme 2. Structural Formula of the Macrocyclic Ligand L

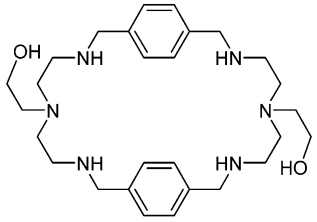

In the past studies, the single macrocyclic (monocyclic) ligands show the favorable advantage for the stabilization of the imidazolate bridge in imidazolate-bridged dicopper(II) complexes; thus, some attempts have been made to use a single macrocyclic ligand to synthesize imidazolate-bridged heterodinuclear Cu(II)−Zn(II) complexes.[4g,8,19] Nevertheless, no such example has been well documented until now. Recently, we designed and synthesized a new single macrocyclic ligand with two flexible hydroxyethyl pendants, L (L = 3,6,9,16,19,22-hexaaza-6,19-bis(2-hydroxyethyl)tricyclo-[22,2,2,2^{11,14}]triaconta-1,11,13,24,27,29-hexaene, as shown in Scheme 2). The macrocyclic ligand L bears both rigidity and flexibility, and the flexible hydroxyethyl arms may be expected to adapt to the different requirement of the configuration for both copper and zinc sites, as well as the proper basicity for copper, zinc ions, and imidazole. Furthermore, the oxygen atom of the hydroxyethyl arms may mimic the role of the water molecule bound to the copper site of Cu_2,Zn_2−SOD. Using the ligand L, we have obtained a new imidazolate-bridged dicopper(II) complex (**1**) and a novel imidazolate-bridged heterodinuclear copper(II)−zinc(II) complex (**2**).[20] In this paper, we present the synthesis, X-ray crystal structures, the results of magnetic susceptibility, ESR, and electronic spectroscopic investigations, and the electrochemistry of the two imidazolate-bridged complexes.

Experimental Section

Materials. All reagents were obtained from commercial suppliers and used without further purification unless otherwise noted. Solvents were purified by standard methods before use. The macrocyclic ligand L was prepared by the procedure described previously.[21]

Physical Measurements. Elemental analysis for C, H, and N was performed on a Perkin-Elmer 240C elemental analyzer, and the contents of metal ions were analyzed on a HOBIN YVON

(3) Ellerby, L. M.; Cabelli, D. E.; Graden, J. A.; Valentine, J. S. *J. Am. Chem. Soc.* **1996**, *118*, 6556.
(4) (a) Kolks, G.; Frihart, C. R.; Rabinowitz, H. N.; Lippard, S. J. *J. Am. Chem. Soc.* **1976**, *98*, 5720. (b) O'Young, C.-L.; Dewan, J. C.; Lilienthal, H. R.; Lippard, S. J. *J. Am. Chem. Soc.* **1978**, *100*, 7291. (c) Coughlin, P. K.; Dewan, J. C.; Lippard, S. J.; Watanabe, E.; Lehn, J.-M. *J. Am. Chem. Soc.* **1979**, *101*, 265. (d) Davis, W. M.; Dewan, J. C.; Lippard, S. J. *Inorg. Chem.* **1981**, *20*, 2933. (e) Kolks, G.; Lippard, S. J.; Waszczak, J. V.; Lilienthal, H. R. *J. Am. Chem. Soc.* **1982**, *104*, 717. (f) Coughlin, P. K.; Martin, A. E.; Dewan, J. C.; Watanabe, E.; Bulkowski, J. E.; Lehn, J.-M.; Lippard, S. J. *Inorg. Chem.* **1984**, *23*, 1004. (g) Coughlin, P. K.; Lippard, S. J. *Inorg. Chem.* **1984**, *23*, 1446.
(5) Drew, M. G. B.; Cairns, C.; Lavery, A.; Nelson, S. M. *J. Chem. Soc., Chem. Commun.* **1980**, 1122.
(6) Drew, M. G. B.; McCann, S. M.; Nelson, S. M. *J. Chem. Soc., Dalton Trans.* **1981**, 1868.
(7) Weser, U.; Schubotz, L. M.; Lengfelder, E. *J. Mol. Catal.* **1981**, *13*, 249.
(8) Strotkamp, K. G.; Lippard, S. J. *Acc. Chem. Res.* **1982**, *15*, 318.
(9) Hendricks, H. M. J.; Birker, P. J. W. L.; Verschoor, G. C.; Reedjik, J. *J. Chem. Soc.; Dalton Trans.* **1982**, 623.
(10) Drew, M. G. B.; Nelson, S. M.; Reedijk, J. *Inorg. Chim. Acta* **1982**, *64*, L189.
(11) Gartner, A.; Weser, U. *Top. Curr. Chem.* **1986**, *132*, 1.
(12) Costes, J.-P.; Serra, J.-F.; Dahan. F.; Laurent, J.-P. *Inorg. Chem.* **1986**, *25*, 2790.
(13) Salata, C. A.; Youinou, M.-T.; Burrows, C. J. *J. Am. Chem. Soc.* **1989**, *111*, 9278.
(14) Salata, C. A.; Youinou, M.-T.; Burrows, C. J. *Inorg. Chem.* **1991**, *30*, 3454.
(15) Kimura, E.; Kurogi, Y.; Shionoya, M.; Shiro, M. *Inorg. Chem.* **1991**, *30*, 4524.
(16) Murphy, B. P. *Coord. Chem. Rev.* **1993**, *124*, 63.
(17) Tabbì, G.; Driessen, W. L.; Reedijk, J.; Bonomo, R. P.; Veldman, N.; Spek, A. L. *Inorg. Chem.* **1997**, *36*, 1168.
(18) (a) Pierre, J. L.; Chautemps, P.; Refaif, S.; Beguin, C.; Marzouki, A. E.; Serratrice, G.; Saint-Aman, E.; Rey, P. *J. Am. Chem. Soc.* **1995**, *117*, 1965 and references cited therein. (b) Ohtsu, H.; Shimazaki, Y.; Odani, A.; Yamauchi, O.; Mori, W.; Itoh, S.; Fukuzumi, S. *J. Am. Chem. Soc.* **2000**, *122*, 5733. (c) Lu, Q.; Luo, Q. H.; Dai, A. B.; Zhou, Z. Y.; Hu, G. Z. *J. Chem. Soc., Chem. Commun.* **1990**, 1429. (d) Mao, Z.; Chen, D.; Tang, W.; Yu, K.; Liu, L. *Polyhedron* **1992**, *11*, 191. (e) Mao, Z.-W.; Chen, M.-Q.; Tan, X.-S.; Liu, J.; Tang, W.-X. *Inorg. Chem.* **1995**, *34*, 2889.
(19) Zhu, H.-L.; Zheng, L.-M.; Fu, D.-G.; Huang, P.; Bu, W.-M.; Tang, W.-X. *Inorg. Chim. Acta* **1999**, *287*, 52.
(20) For a preliminary communication, see: Li, S.; Li, D.; Yang, D.; Li, Y.; Huang, J.; Yu, K.; Wen, X. *Chem. Commun.* **2003**, 880.
(21) Li, S.-A.; Xia, J.; Yang, D.-X.; Xu, Y.; Li, D.-F.; Wu, M.-F.; Tang, W.-X. *Inorg. Chem.* **2002**, *41*, 1807.

JY38S ICP spectrometer. The polycrystalline powder ESR spectra at room temperature and the 110 K ESR spectra in frozen 50% aqueous dimethyl sulfoxide (DMSO) solutions as a function of pH were recorded with a Bruker 200D-SRC spectrometer employing X-band radiation and a cylindrical cavity with 100 kHz magnetic field modulation. Calibrations of the microwave frequency were performed with an EIP845A microwave frequency counter. The magnetic susceptibilities of complex **1** were obtained on polycrystalline samples using a Model MagLab system 2000 magnetometer in the temperature range 2−300 K with an applied field of 1.0 T. The experimental susceptibilities were corrected for the sample holder and the diamagnetism contributions estimated from Pascal's constants. Effective magnetic moments were calculated using the equation $\mu_{eff} = 2.828(\chi_M T)^{1/2}$, where χ_M is the molar magnetic susceptibility.

[(CuimCu)L](ClO$_4$)$_3$·0.5H$_2$O (1). To a methanol solution (5 mL) of Cu(ClO$_4$)$_2$·6H$_2$O (0.1025 g, 0.277 mmol) was added a solution of imidazole (0.0188 g, 0.277 mmol) in methanol (2 mL) dropwise over 10 min. The resulting blue solution was stirred for 0.5 h and then was added dropwise to a methanol solution (10 mL, pH ca. 9) of L (0.066 g, 0.133 mmol). Afterward, the resultant deep-blue solution (pH ca. 6) was stirred for another 0.5 h at room temperature and led to a blue precipitate, which was filtered and washed with methanol and ether (yield: 91%). The blue precipitate was dissolved in 3 mL of CH$_3$CN and recrystallized by slow diffusion of methanol at ambient temperature. Block, blue crystals were obtained after several days. Anal. Calcd for $C_{31}H_{50}Cl_3Cu_2N_8O_{14.5}$: C, 37.23%; H, 5.04%; N, 10.63%. Found: C, 37.66%; H, 4.93%; N, 10.85%.

[(CuimZnL$_{-2H}$)(CuimZnL$_{-H}$)](ClO$_4$)$_3$ (2). To a solution of 0.141 g (0.283 mmol) of L in 2 mL of water were added 0.105 g (0.283 mmol) of Zn(ClO$_4$)$_2$·6H$_2$O in 2 mL of water and 0.105 g (0.283 mmol) of Cu(ClO$_4$)$_2$·6H$_2$O in 2 mL of water with stirring. After 30 min, a solution of 0.0193 g (0.283 mmol) of imidazole in 2 mL of water was added. Acetonitrile was added dropwise to the described solution until the resultant small amount of blue precipitate was dissolved. Then, the pH value of the resulting solution was slowly and carefully adjusted to ca. 9.5 with 0.1 M NaOH solution with continuous stirring, and the solution turned from blue to green. Platelet, green crystals were obtained by slow evaporation of this solution in air at 15−20 °C for several days (yield: 74%). The crystals effloresce quickly in air when they were separated from the mother solution. Anal. Calcd for $C_{62}H_{87}Cl_3Cu_2N_{16}O_{16}Zn_2$: C, 44.41; H, 5.23; N, 13.37; Cu, 7.58; Zn, 7.80%. Found: C, 44.36; H, 5.29; N, 13.42; Cu, 7.62; Zn, 7.76%.

Caution! *Perchlorate salts of compounds containing organic ligands are potentially explosive, especially when heated or bumped. Only small quantities of these compounds should be prepared and handled behind suitable protective shields.*

X-ray Structure Determination. Intensity data for **1** were collected on a Siemens P4 four-circle diffractometer with monochromated Mo Kα radiation (λ = 0.71073 Å) using ω scans at room temperature. Data were corrected for Lorentz-polarization effects during data reduction using XSCANS,[22] and a semiempirical absorption correction from ψ-scans was applied. The structure was solved by direct methods and refined on F^2 using the SHELXTL[23] software package. One of the perchlorate anions (Cl3, O11, O12, O13, and O14) was disordered over two positions, each refined at half-occupancy. Except two disordered atoms (O13 and O14), the other non-hydrogen atoms were refined anisotropically by full-matrix least-squares. The C−H, N−H, and O−H atoms were computed and refined isotropically using a riding model. For complex **2**, a green single crystal suitable for X-ray analysis was enveloped in a glass capillary and used to collect diffraction data on a Bruker SMART CCD diffractometer equipped with monochromated Mo Kα radiation (λ = 0.71073 Å) at room temperature. A total of 23946 reflections were collected in the range $1.82 \le \theta \le 25.00°$, of which 16118 were unique reflections and 9292 with $I \ge 2\sigma(I)$ were considered to be observed. The data integration and empirical absorption corrections were applied with the SAINT[24] and SADABS[25] programs, respectively. The structure was solved by direct methods and refined on F^2 using the SHELXTL software package. All non-hydrogen atoms were refined anisotropically by full-matrix least-squares. Apart from H1 of O3, found from the difference Fourier map, the other C−H and N−H atoms were computed and refined isotropically using a riding model. Summaries of the fundamental crystal data and experiment parameters for the structure determination of complexes **1** and **2** are listed in Table 1.

Table 1. Summary of X-ray Crystallographic Data for [(CuimCu)L](ClO$_4$)$_3$·0.5H$_2$O (**1**) and [(CuimZnL$_{-2H}$)(CuimZnL$_{-H}$)](ClO$_4$)$_3$ (**2**)

	1	**2**
empirical formula	$C_{31}H_{50}N_8O_{14.5}Cl_3Cu_2$	$C_{62}H_{95}N_{16}O_{16}Cl_3Cu_2Zn_2$
fw	1000.22	1684.71
cryst syst	orthorhombic	triclinic
space group	*Pbca*	$P\bar{1}$
a, Å	18.709(4)	14.172(2)
b, Å	19.238(4)	16.673(2)
c, Å	23.100(5)	21.284(3)
α, deg	90	74.110(10)
β, deg	90	75.200(10)
γ, deg	90	82.220(10)
V, Å^3	8314(3)	4665.0(11)
Z	8	2
F(000)	4108	1752
D_{calcd}, g/cm^3	1.597	1.199
crystal size, mm^3	0.32 × 0.30 × 0.28	0.3 × 0.2 × 0.2
μ(Mo Kα), mm^{-1}	1.290	1.103
diffractometer	Siemens P4	Bruker APEX SMART CCD
radiation	Mo Kα (0.71073 Å)	Mo Kα (0.71073 Å)
reflns collected/ unique	8474/7303 (R_{int} = 0.0216)	23946/16118 (R_{int} = 0.0325)
reflns obsd [$I > 2\sigma(I)$]	2476	9292
R1 [$I > 2\sigma(I)$]	0.0735	0.0516
wR2 [$I > 2\sigma(I)$]	0.1679	0.1220

Electrochemistry. Redox potentials of complexes **1** and **2** (1.0 mM) in dried *N*,*N*-dimethylformamide (DMF) containing 0.1 M tetra-*n*-butylammonium perchlorate (TBAP) as supporting electrolyte were determined at room temperature by cyclic voltammetry using a conventional three-electrode system under nitrogen atmosphere and a BAS 100A electrochemical analyzer. A glassy carbon electrode and a platinum wire were used as the working electrode and the counter electrode, respectively. A saturated calomel electrode (SCE), separated from the test solution by the electrolytic solution sandwiched between two fritted disks and calibrated using the ferrocene/ferrocenium redox couple, was used as the reference electrode.

SOD Activities Determination. Superoxide anions were generated by the hypoxanthine−xanthine oxidase reaction as described in the literature. The SOD activity was evaluated using the nitro blue tetrazolium (NBT) assay.[17,26]

(22) *XSCANS*, version 2.1; Siemens Analytical X-ray Instruments: Madison, WI, 1994.
(23) Sheldrick, G. M. *SHELXTL*, version 5.1; Bruker AXS Inc.: Madison, WI, 1998.
(24) *SAINT, Data Integration Software*, version 4.0; Bruker AXS Inc.: Madison, WI, 1997.
(25) Sheldrick, G. M. *SADABS, Empirical Absorption Correction Program*, version 2.01: University of Göttingen: Göttingen, Germany, 1996.
(26) Bielski, B. H. J.; Shiue, G. G.; Bajuk, S. *J. Phys. Chem.* **1980**, *84*, 830.

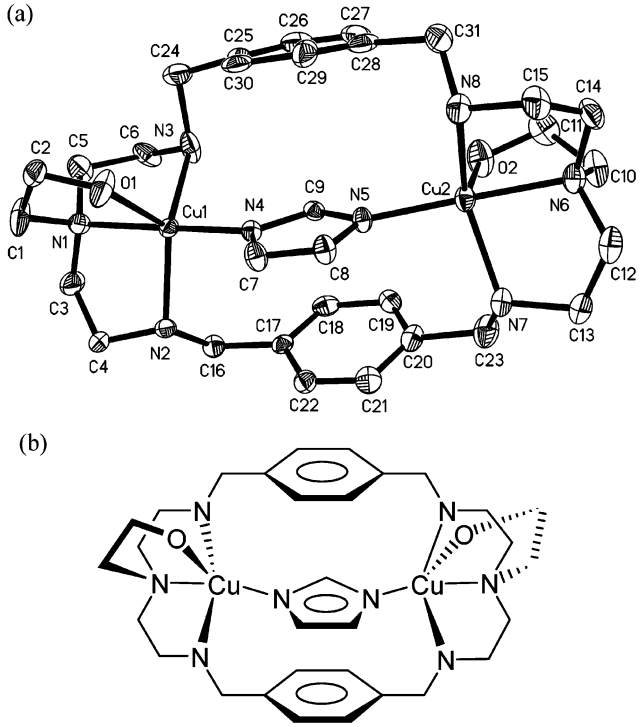

Figure 1. (a) ORTEP drawing of the cation $[(CuimCu)L]^{3+}$ of **1**, with thermal ellipsoids drawn at the 30% probability level. (b) Schematic representation of the cation.

Results and Discussion

Crystal Structures. Molecular structures of the dinuclear complexes **1** and **2**, together with their schematic representations, are shown in Figures 1 and 2, respectively. Selected bond distances and angles are listed in Tables 2 and 3, respectively.

$[(CuimCu)L](ClO_4)_3 \cdot 0.5H_2O$ (1). The molecular structure of **1** clearly shows that it is an imidazolate-bridged homodinuclear Cu(II)−Cu(II) complex. In the asymmetric unit, there is a $[(CuimCu)L]^{3+}$ cation in which two copper atoms are bridged by an imidazolate anion. Each copper atom is coordinated by an N4O environment (three nitrogen and one oxygen atoms from the ligand L, one nitrogen atom from imidazolate) with a coordination geometry between trigonal bipyramid (TBP) and tetragonal pyramid (TP). The degree of distortion (Δ) from TBP to TP can be estimated according to the method of Muetterties[27] and Galy.[28] Analysis of the Cu coordination polyhedra gives the values of $\Delta = 0.38$ for Cu1 and $\Delta = 0.60$ for Cu2, indicating a coordination geometry of distorted trigonal bipyramid (TBP) for Cu1 and distorted tetragonal pyramid (TP) for Cu2, respectively. The Cu1 deviates 0.240 (7) Å from the mean trigonal plane determined by O1, N2, and N3 toward the imidazolate ring, while the axial positions are occupied by N1 of the macrocycle and N4 of the bridging imidazolate with the angle N1−Cu1−N4 = 171.4(3)°, and bond lengths Cu1−N1 and Cu1−N4 are 2.055(8) and 1.966(7) Å, respectively. For Cu2, the apical position of the TP coordination geometry is occupied by O2 with bond length Cu2−O2 = 2.182(8) Å, and Cu2 deviates 0.335(6) Å from the basal plane determined by N5, N6, N7, and N8 with the average Cu−N distances of 2.049(8) Å. Distance between the two imidazolate-bridged Cu(II) ions is 5.999(2) Å, which is similar to those observed in other imidazolate-bridged dicopper(II) complexes. The two copper ions are almost coplanar with the imidazolate ring, only out of the plane with 0.207(5) Å for Cu1 and 0.045(3) Å for Cu2, respectively. The bridged imidazolate ring partially sandwiches between the two phenyl rings of the macrocyclic ligand, and the imidazolate ring is approximately parallel to the two phenyl rings (14.0(4)° for C17−C22 plane and 9.0(5)° for C25−C30 plane). The distance between the centers of the imidazolate ring and phenyl rings are 3.34 Å for C17−C22 plane and 3.59 Å for C25−C30 plane, indicating $\pi-\pi$ stacking interaction between those rings. Additionally, the two hydroxyethyl groups are located at the different sides of the plane defined by nitrogen atoms of the macrocyclic ligand, forming a chairlike (*anti*) conformation.

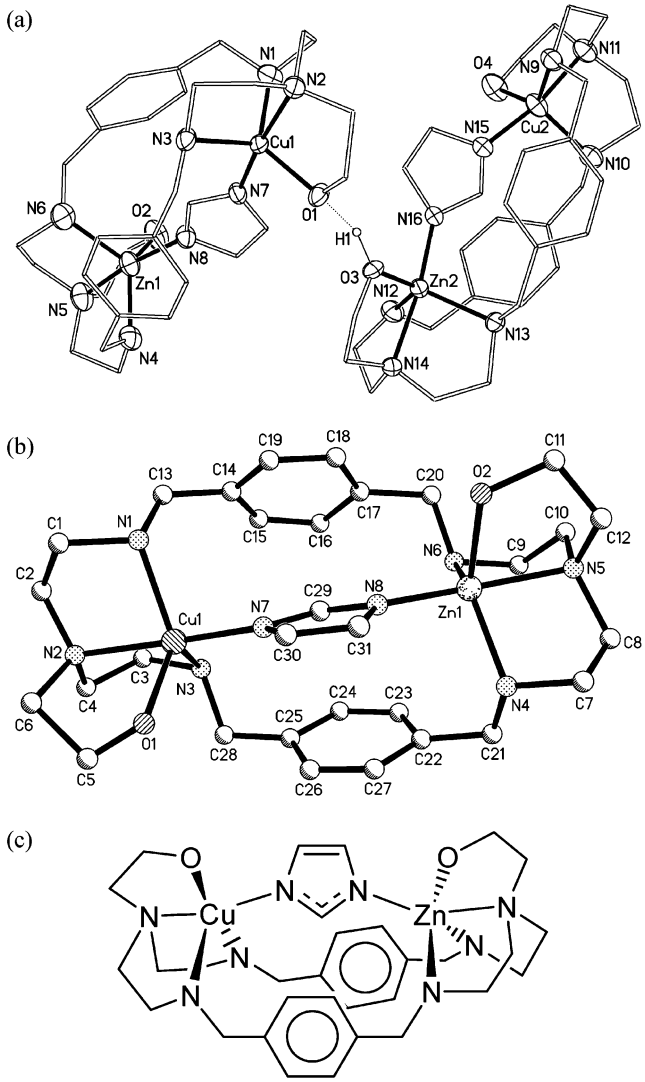

Figure 2. (a) Molecular structure of the Cu(II)−Zn(II) heterodinuclear complex $[(CuimZnL_{-2H})(CuimZnL_{-H})](ClO_4)_3$ (**2**). (b) Molecular structure of cation **2A**, $[(CuimZn)L_{-2H}]^{3+}$. (c) Schematic representation of this cation.

(27) Mutterties, E. L.; Guggenberger, L. J. *J. Am. Chem. Soc.* **1974**, *96*, 1748.
(28) Galy, J.; Bonnet, J. I.; Anderson, S. *Acta Chem. Scand.* **1979**, *A33*, 383.

Table 2. Selected Bond Lengths (Å) and Angles (deg) for $[(CuimCu)L](ClO_4)_3 \cdot 0.5H_2O$ (**1**)

Cu(1)−N(1)	2.055(8)	Cu(2)−N(5)	1.967(7)
Cu(1)−N(2)	2.111(7)	Cu(2)−N(6)	2.049(8)
Cu(1)−N(3)	2.107(8)	Cu(2)−N(7)	2.101(9)
Cu(1)−N(4)	1.966(7)	Cu(2)−N(8)	2.079(8)
Cu(1)−O(1)	2.199(8)	Cu(2)−O(2)	2.182(8)
N(1)−Cu(1)−N(2)	84.2(3)	N(5)−Cu(2)−O(2)	105.8(3)
N(1)−Cu(1)−N(3)	83.9(3)	N(5)−Cu(2)−N(6)	173.7(3)
N(1)−Cu(1)−O(1)	80.5(3)	N(5)−Cu(2)−N(7)	97.9(3)
N(2)−Cu(1)−O(1)	119.7(3)	N(5)−Cu(2)−N(8)	93.7(3)
N(3)−Cu(1)−O(1)	105.8(4)	N(6)−Cu(2)−N(7)	82.0(3)
N(3)−Cu(1)−N(2)	130.0(4)	N(6)−Cu(2)−N(8)	83.2(4)
N(4)−Cu(1)−O(1)	91.3(3)	N(6)−Cu(2)−O(2)	80.4(3)
N(4)−Cu(1)−N(1)	171.4(3)	N(7)−Cu(2)−O(2)	100.7(4)
N(4)−Cu(1)−N(2)	97.9(3)	N(8)−Cu(2)−O(2)	106.9(4)
N(4)−Cu(1)−N(3)	100.9(3)	N(8)−Cu(2)−N(7)	145.8(4)
C(7)−N(4)−Cu(1)	125.1(7)	C(8)−N(5)−Cu(2)	124.7(6)

Table 3. Selected Bond Lengths (Å) and Angles (deg) for $[(CuimZnL_{-2H})(CuimZnL_{-H})](ClO_4)_3$ (**2**)

cation **2A**		cation **2B**	
Cu(1)−O(1)	2.020(3)	Cu(2)−O(4)	2.120(3)
Cu(1)−N(1)	2.131(4)	Cu(2)−N(9)	2.117(3)
Cu(1)−N(2)	2.144(3)	Cu(2)−N(10)	2.109(4)
Cu(1)−N(3)	2.135(3)	Cu(2)−N(11)	2.119(4)
Cu(1)−N(7)	1.971(3)	Cu(2)−N(15)	1.910(3)
Zn(1)−O(2)	2.101(3)	Zn(2)−O(3)	2.000(3)
Zn(1)−N(4)	2.086(4)	Zn(2)−N(12)	2.146(4)
Zn(1)−N(5)	2.093(4)	Zn(2)−N(13)	2.150(3)
Zn(1)−N(6)	2.201(4)	Zn(2)−N(14)	2.149(3)
Zn(1)−N(8)	1.914(3)	Zn(2)−N(16)	1.933(3)
O(1)−Cu(1)−N(1)	127.53(13)	O(4)−Cu(2)−N(9)	129.72(14)
O(1)−Cu(1)−N(2)	81.17(12)	N(10)−Cu(2)−O(4)	104.95(15)
O(1)−Cu(1)−N(3)	112.25(13)	N(10)−Cu(2)−N(9)	119.77(14)
N(1)−Cu(1)−N(2)	81.23(14)	N(10)−Cu(2)−N(11)	84.44(15)
N(1)−Cu(1)−N(3)	113.89(14)	N(11)−Cu(2)−O(4)	80.31(15)
N(2)−Cu(1)−N(3)	82.68(13)	N(11)−Cu(2)−N(9)	82.24(15)
N(7)−Cu(1)−O(1)	94.83(12)	N(12)−Zn(2)−N(13)	115.07(13)
N(7)−Cu(1)−N(1)	97.16(14)	N(14)−Zn(2)−N(12)	82.13(13)
N(7)−Cu(1)−N(3)	103.88(12)	N(14)−Zn(2)−N(13)	81.51(12)
N(7)−Cu(1)−N(2)	173.28(13)	N(15)−Cu(2)−O(4)	92.40(14)
N(4)−Zn(1)−O(2)	132.28(15)	N(15)−Cu(2)−N(9)	97.26(14)
N(4)−Zn(1)−N(5)	82.30(17)	N(15)−Cu(2)−N(10)	104.42(15)
N(4)−Zn(1)−N(6)	115.64(15)	N(15)−Cu(2)−N(11)	169.82(16)
N(5)−Zn(1)−N(6)	85.56(16)	N(16)−Zn(2)−O(3)	94.07(13)
N(5)−Zn(1)−O(2)	79.04(16)	N(16)−Zn(2)−N(12)	98.39(14)
N(8)−Zn(1)−O(2)	93.11(13)	N(16)−Zn(2)−N(13)	104.97(12)
N(8)−Zn(1)−N(4)	97.11(14)	N(16)−Zn(2)−N(14)	172.38(12)
N(8)−Zn(1)−N(5)	168.41(16)	O(3)−Zn(2)−N(12)	126.48(13)
N(8)−Zn(1)−N(6)	104.96(14)	O(3)−Zn(2)−N(13)	111.31(12)
O(2)−Zn(1)−N(6)	106.24(15)	O(3)−Zn(2)−N(14)	79.66(12)

$[(CuimZnL_{-2H})(CuimZnL_{-H})](ClO_4)_3$ (2). Compared to **1**, the structure of **2** is remarkably different. The asymmetric unit contains two Cu(II)−Zn(II) heterodinuclear cations, $[(CuimZn)L_{-2H}]^+$ (cation **2A**) and $[(CuimZn)L_{-H}]^{2+}$ (cation **2B**),[29] joined together through hydrogen bonding O1···H1−O3 [O1···O3, 2.403(3) Å; O1···H1−O3, 152(4)°], as well as three perchlorate anions (Figure 2a), and the two heterodinuclear cations form a dihedral angle of 57.9(1)° based on the two Cu−im−Zn planes. The two cations are basically similar but somewhat different with respect to the coordination geometry, bond lengths, and angles. Analysis of the Cu and Zn coordination geometry provides the values of Δ = 0.31/0.31 for Cu1/Cu2 and Δ = 0.15/0.12 for Zn1/Zn2, respectively. The results indicate that the coordination geometries around the copper and zinc atoms are all distorted trigonal bipyramid (TBP) and the distortion of Cu1/Cu2 is more obvious than that of Zn1/Zn2, which is consistent with the tendency that the Zn(II) ion favors the trigonal bipyramidal coordination geometry much more than the Cu(II) ion.[18b] In cation **2A**,[30] both Cu(II) and Zn(II) atoms are coordinated in an N4O environment, in which three nitrogen and one oxygen atoms (N1, N2, N3, and O1 for Cu1; N4, N5, N6, and O2 for Zn1) are from ligand L, and one nitrogen atom is from imidazolate (N7 for Cu1 and N8 for Zn1) (Figure 2b). The Cu1 atom is located at 0.218(1) Å out of the mean trigonal equatorial plane defined by N1, N3, and O1 atoms toward imidazolate; the axial positions are occupied by two nitrogen atoms from the macrocycle and imidazolate ring, respectively, with Cu1−N2 = 2.144(3) Å and Cu1−N7 = 1.971(3) Å. While the Zn1 atom is displaced by 0.213(1) Å toward N8 from the mean plane, the two apical sites are coordinated by two nitrogen atoms from the macrocycle and imidazolate ring, respectively, with Zn1−N5 = 2.093(4) Å and Zn1−N8 = 1.914(3) Å. Distance between the imidazolate-bridged Cu(II) and Zn(II) ions is 5.950(1) Å (for cation **2B**, the distance is 5.939(1) Å), which is slightly shorter than that in Cu_2,Zn_2-SOD (Cu···Zn = 6.3 Å).

The most obvious discrepancies between complex **1** and cation **2A**/**2B** exist in the conformation of the macrocycle with two pendants, the conformation of the two phenyl spacers, and the position of the bridged imidazolate ring. The two phenyl groups in cation **2A** are not parallel to each other but have a dihedral angle of 51.2(1)°, and the imidazolate ring is not parallel to the phenyl ring C14−C19 with dihedral angles of 38.7(2)°. Moreover, the imidazolate ring is basically carried on a "boat" constructed by the macrocycle with two hydroxyethyl arms, as well as the Cu(II) and Zn(II) ions. It is worth noting that the two hydroxyethyl arms in **2** are located on the same sides, forming a boatlike (*syn*) conformation, but a chairlike conformation in **1**. This difference in the conformation of the ligand with two arms can only be accomplished by stereochemical inversion at one (or more) of the nitrogen atoms (at least, one of the two tertiary nitrogen atoms) of the free macrocyclic ligand in the formation of the complexes.[31]

The remarkable differences between complexes **1** and **2** provide substantial evidence for the formation of the heterodinuclear imidazolate-bridged Cu(II)−Zn(II) complex. The changes in the bond lengths and angles, the conformation of macrocyclic ligand L, and the position of imidazolate rings demonstrate that the overall ligand, especially the two flexible hydroxyethyl arms, possesses a good adjustability for the different configuration requirements for both Cu(II) and Zn(II) metal ions in the course of the formation of the complexes.

(29) L_{-H} and L_{-2H} represent the ligand L deprotonated one and two protons from the hydroxyethyl pendants, respectively.

(30) For the sake of the similarity of the two cations, **2A** and **2B**, we only described the structure of cation **2A** in the following.

(31) Sutherland, I. O. In *Comprehensive Organic Chemistry: The Synthesis and Reactions of Organic Compounds, Vol. II, Nitrogen, Compounds, Carboxylic Acids, Phosphorus Compounds*, 1st ed.; Barton, D., Ollis, W. D., Eds.; Pergamon Press: Exeter, U.K., 1979; pp 26−29.

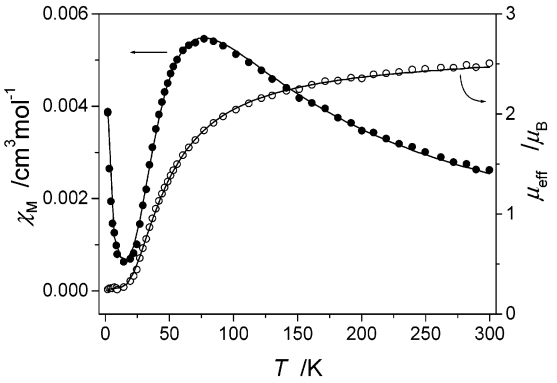

Figure 3. Temperature dependence of the magnetic susceptibility for complex **1** in the form χ_M (●) and μ_{eff} (○) vs *T*. The solid lines result from a least-squares fit according to eq 1 (see text).

Magnetic Properties. The temperature dependence of the magnetic susceptibility for dicopper(II) compound **1** was measured in the range 2−300 K. The magnetic behavior is depicted in Figure 3 in the forms of the magnetic molar susceptibility (χ_M) and the effective magnetic moment (μ_{eff}) versus *T*. When the temperature decreases, the value of χ_M increases continuously, reaches a maximum around 78 K, and then falls to a minimum at 14 K. This behavior, together with a monotonic decreasing of μ_{eff} upon cooling, is characteristic of antiferromagnetic exchange interaction between two imidazolate-bridged Cu(II) ions. The abrupt rise of χ_M below 14 K is due to small amounts of paramagnetic impurities such as Cu^{2+}. The susceptibility data were fitted to the modified Bleaney−Bowers equation for exchange-coupled pairs of copper(II) ions (eq 1),[32] where $-2J$ represents the magnetic exchange parameter, *g* is the Landé factor, χ_{TIP} is temperature-independent paramagnetism, and *p* is the molar fraction of paramagnetic impurity.

$$\chi_M = (1-p)\frac{2Ng^2\beta^2}{kT}[3+\exp(-2J/kT)]^{-1} + p\frac{2Ng^2\beta^2S(S+1)}{3kT} + \chi_{TIP} \quad (1)$$

The best fit for χ_M versus *T* in the range 2−300 K leads to the following parameters: $-2J = 86.4(3)$ cm^{-1}, $g = 2.10(1)$, $\chi_{TIP} = 1.03(3) \times 10^{-4}$ cm^3·mol^{-1}, $p = 9.00(1) \times 10^{-3}$, and $R = 5.46 \times 10^{-9}$ ($R = \sum[(\chi_M)_{obs} - (\chi_M)_{cacld}]^2/\sum[(\chi_M)_{obs}]^2$) (as shown in Figure 3).

The $-2J$ (86.4 cm^{-1}) value falls in the range (0−163 cm^{-1}) for most imidazolate-bridged dicopper(II) complexes[8] and is very close to that (88 cm^{-1}) of the reported dicopper(II) compound of the cryptand L′, [(Cu(im)Cu)L′](ClO$_4$)$_3$, **5**, but is larger than the reported value (52.0 cm^{-1}) for Cu$_2$,Cu$_2$-SOD.[18a]

ESR Studies. The X-band ESR spectra of complex **1** in polycrystalline powder at room temperature and in frozen water/DMSO (1:1) solution at 110 K are shown in Figure 4. The spectra exhibit the typical features for antiferromagnetic coupled imidazolate-bridged dicopper(II) complexes: (i) For the frozen solution spectrum, the $\Delta M_S = \pm 1$ zero-field splitting region shows two broad signals (ca. 2870 and 3650 G) centered at $g = 2.11$ and a flattened signal at ca. 2470 G, which is characteristic of zero-field splitting effects on $g_{\|}$ and $g_{\perp}$ signals. (ii) In both spectra, the $\Delta M_S = \pm 2$ half-field signals are observed at about 1500 G with $g_{hf} = 4.3$, especially the spectrum in frozen solution which displays the expected seven hyperfine lines to give a splitting of 61.3 G. These characters reveal clearly the presence of magnetic interaction between two copper(II) ions through the imidazolate bridge. By analyzing spectrum b, we obtained the following values: $|D| = 0.073$ cm^{-1}, $g_{\|} = 2.22$, and $g_{\perp} = 2.07$, where *D* is the zero-field splitting parameter. These values are consistent with other reported imidazolate-bridged dinuclear Cu(II) complexes.[18a]

The X-band ESR spectra of complex **2** in polycrystalline powder at room temperature and in frozen water/DMSO (1:1) solution at 110 K are shown in Figure 5. The spectrum in the solid sample only shows a simple isotropic signal at $g_{iso} = 2.05$, while the frozen-solution spectrum gives several well-defined signals at the center field, typical of the mononuclear copper(II) ions in a trigonal bipyramidal environment with a d_{z^2} ground state,[33] which is consistent with the X-ray structure result already discussed. The measured values are

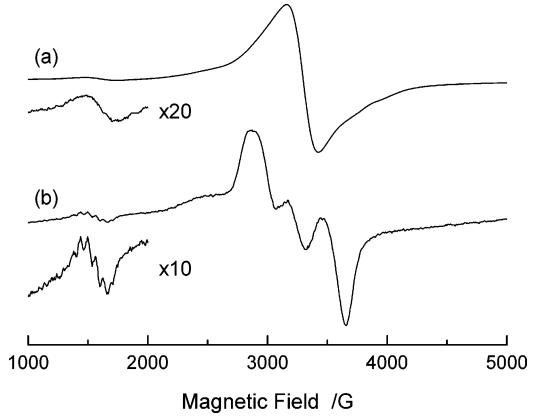

Figure 4. ESR spectra for complex **1**: (a) polycrystalline powder at room temperature and (b) frozen water/DMSO (1:1) solution at 110 K.

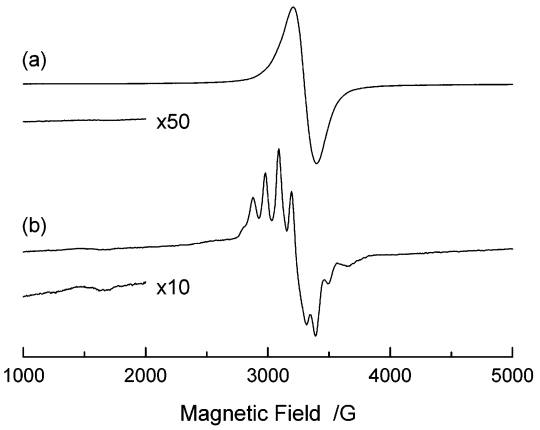

Figure 5. ESR spectra for complex **2**: (a) polycrystalline powder at room temperature and (b) frozen water/DMSO (1:1) solution at 110 K.

(32) Bleaney, B.; Bowers, K. D. *Proc. R. Soc. London, Ser. A* **1952**, *214*, 451.

(33) Bencini, A.; Bertini, I.; Gatteschi, D.; Scozzafava, A. *Inorg. Chem.* **1978**, *17*, 3194.

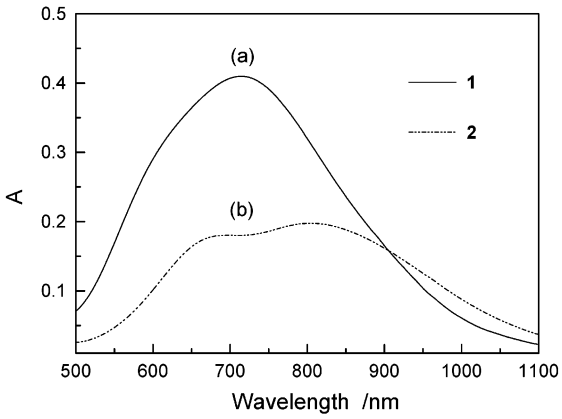

Figure 6. UV−vis spectra of (a) $[(CuimCu)L](ClO_4)_3 \cdot 0.5H_2O$ (**1**, 1.0 mM for a Cu_2 unit) and (b) $[(CuimZnL_{-2H})(CuimZnL_{-H})](ClO_4)_3$ (**2**, 1.0 mM for one CuZn unit) in aqueous solution at 298 K.

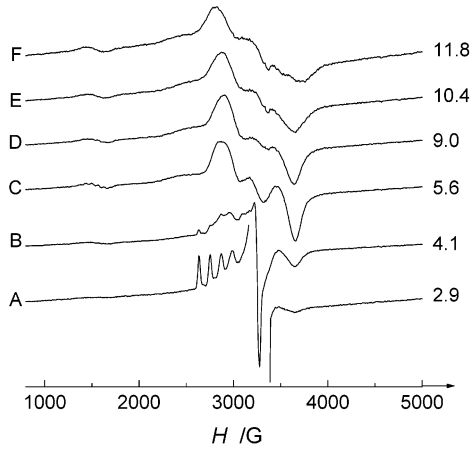

Figure 7. ESR spectra of **1** in frozen water/DMSO solutions (1:1, v/v) at 110 K as a function of pH.

Scheme 3. Proposed Mechanism for the Spectral Changes for High pH Solutions in ESR and UV−Vis Studies

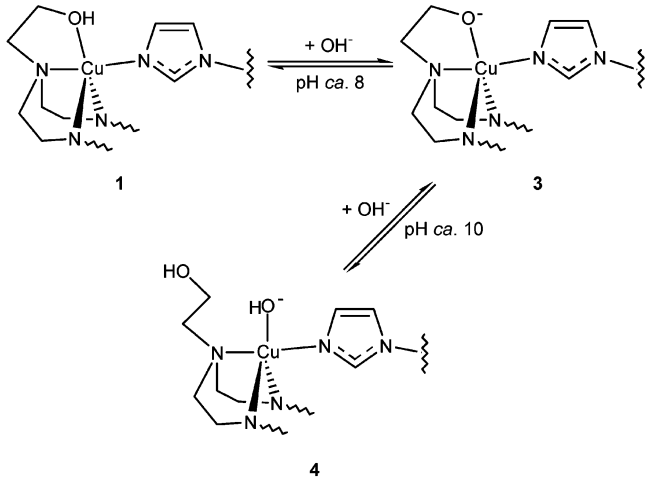

$g_{\|} = 1.94$, $g_{\perp} = 2.23$, $A_{\|} = 116$ G, and $A_{\perp} = -105$ G, which are similar to those of CuX(Me$_6$tren)X (X = Br or I), a mononuclear five-coordinated trigonal bipyramidal copper(II) complex,[34] and the reported imidazolate-bridged Cu−Zn complex, $[CuZn(Me_4bdpi)(CH_3CN)_2]^{3+}$, which possesses a trigonal bipyramidal environment.[18b] Such a spectrum is different from that of Cu_2,Zn_2-SOD ($g_{\|} = 2.26 > g_{\perp} = 2.07$), possessing a distorted square pyramidal geometry around the copper(II) ion. Additionally, when the curves are magnified, a very weak signal at about 1500 G, together with a shoulder at 2800 G in the frozen-solution spectrum, assigned to a very small amount exchanged (Cu−im−Cu) species, can be observed; this signal is not seen in the spectrum of the solid sample even when the curve is magnified 50 times. These results show that the solid sample contains only the Cu−im−Zn species, and that this species is also the major component in aqueous solution.

UV−Vis Spectra. The UV−vis spectrum of complex **1** (1.0 mM for a Cu_2 unit) in water shown in Figure 6a exhibits a broad d−d band centered at 720 nm (ϵ = 409 $mol^{-1} \cdot dm^3 \cdot cm^{-1}$) with a shoulder at 610 nm. The spectrum of complex **2** (1.0 mM for one CuZn unit) in Figure 6b shows two broad bands centered at 680 nm (ϵ = 170 $mol^{-1} \cdot dm^3 \cdot cm^{-1}$) and 820 nm (197 $mol^{-1} \cdot dm^3 \cdot cm^{-1}$) for d−d transitions as expected in trigonal bipyramidal geometry for Cu(II) ions.[35] The electronic spectrum of **2** is different from that of Cu_2,Zn_2-SOD having one band at ca. 680 nm, due to their different coordination geometry around Cu(II) ions. Additionally, the reflectance spectra of complexes **1** and **2** in the solid state show the same broad bands as those in water solution, demonstrating that the structures of **1** and **2** in solution are the same as those in the solid state. Obviously, the results clearly show that the complexes are rather stable, are the main species in water, and give reliable support for the following studies on the solution stability in aqueous solution.

pH Dependence of ESR and UV−Vis Spectra of Complexes 1 and 2. Complex $[(CuimCu)L](ClO_4)_3$ (1). The ESR spectra of complex **1** in frozen 50% aqueous DMSO solution at 110 K as a function of pH are displayed in Figure 7. The spectra of the complex (C−F), in the range 5.6 ≤ pH ≤ 11.8, exhibit almost the same signals as that of complex **1**, implying that the imidazolate-bridged dicopper(II) cores are still stable in these solutions. The slight change in spectra C−F may be caused by the deprotonation of the alcohol arms and by the competitive substitution of the resultant alkoxide groups with OH^- anions at high pH solutions (as depicted in Scheme 3 and discussed in following paragraphs). When pH = 4.1, another signal is imposed, implying the breakage of the imidazolate bridge, and at pH = 2.9, the spectrum exhibits only the signals of free Cu(II), indicative of the complete protonation of the macrocycle.

A further study on the pH-dependent UV−vis spectrometry for **1** in either water or water/DMSO (1:1) solution gave similar results. In water, from pH 4.64 to 9.92, the spectra all show a broad band at 720 nm with a shoulder at about 610 nm, which is the same as that of **1** dissolved in water solution. At pH = 1.98, the d−d transition band for free Cu(II) ion in aqueous solution was observed at about 800 nm, revealing that complex **1** is completely dissociated.

The study of the formation of complex **1** was carried out by UV−vis spectrometry starting from the previous aqueous solution obtained at pH 1.98. The visible spectra (500−1100

(34) Barbucci, R.; Bencini, A.; Gatteschi, D. *Inorg. Chem.* **1977**, *16*, 2117.
(35) Hathaway, B. J. *J. Chem. Soc., Dalton Trans.* **1972**, 1196.

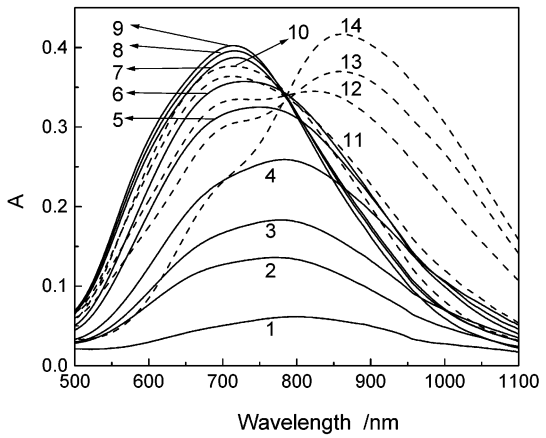

Figure 8. Electronic spectra of **1** in aqueous solution recorded as a function of pH. From 1 to 9 for solid lines: pH = 1.98, 3.22, 3.90, 4.22, 4.58, 4.81, 5.10, 6.35, and 7.62. From 10 to 14 for dashed lines: pH = 8.76, 9.88, 10.14, 10.95, and 11.98.

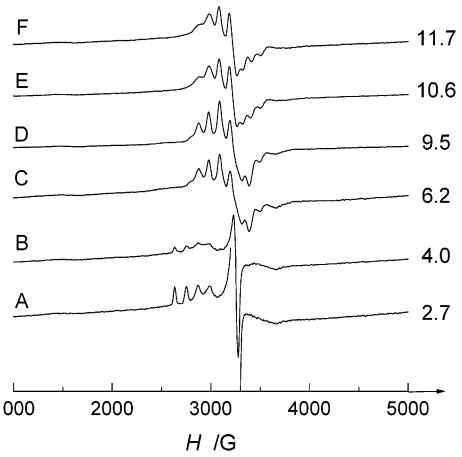

Figure 9. ESR spectra of **2** in frozen water/DMSO solutions (1:1, v/v) at 110 K as a function of pH.

nm) covering the pH range 1.98−11.98 are shown in Figure 8. It can be seen that the spectra in the range 4.81 ≤ pH ≤ 9.88 show similar or the same feature as that of the visible spectrum of **1** dissolved in aqueous solution (Figure 6a), demonstrating clearly the formation of imidazolate-bridged dicopper(II) species above pH 4.81. Thus, complex **1** can be reproduced from an acidic solution on raising the pH to about 5. Our previous titration study on a dicopper(II) complex of this macrocyclic ligand L, $[Cu_2LCl_2]Cl_2 \cdot 5.5H_2O$, has shown that the hydroxyethyl pendants bound to Cu(II) will be deprontonated at pH ca. 8.[21] The similarity of these spectra in such a pH range also implies that the deprotonation of the alcohol arms at pH ca. 8 only brings a very weak perturbation to the coordination environment of copper ions. Moreover, a new peak at 850 nm appears in the spectra above pH = 10.14 and becomes stronger and stronger with the increasing alkalinity of the solution; at the same time, the peak at 720 nm is gradually reduced. This change implies the formation of a new species in the high pH solutions. On the basis of the ESR study, the curves of the high pH solutions exhibit the typical signals for imidazolate-bridged dicopper(II) complexes (Figure 7D−F), illustrating that the major component in these solutions is still an imidazolate-bridged dicopper(II) complex; i.e., the imidazolate bridge is unbroken and is retained in the resultant product. Additionally, Kimura et al. have studied the solution behavior of a zinc(II) complex with an alcohol-pendant cyclen ((1-(2-hydroxyethyl)-1,4,7,10-tetraazacyclododecane), L^1), ZnL^1.[36] The results showed that a monodeprotonated species ZnL^1-OH^-, in which an OH^- group coordinates to the zinc ion instead of the alcohol arm, was considered the most reasonable product at pH above ca. 8. On these bases, the new species as the major component is rationally proposed to be a substitutional product (**4**) of alkoxide arms by OH^- anions above pH 10 (Scheme 3).

Interestingly, when the aqueous solution obtained at pH 11.98 was readjusted to pH ca. 9.8, the peak at 850 nm disappeared, and the spectrum became almost the same as the previous one at pH 9.88. This can be interpreted as the result of the substitution of hydroxyl groups bound to Cu(II) ions with the alkoxide pendants, i.e., the reproduction of the cation $[(CuimCu)L]^+$, **3**, below pH ca. 10 (Scheme 3).

These results demonstrate that the imidazolate-bridged dicopper cation ($[(CuimCu)L]^{3+}$ **1**, **3**, and **4**) is the major component in solution in the range 5 ≤ pH ≤ 12 and the alkoxide pendants will be reversibly substituted by OH^- anions at pH ca. 10.

Complex $[(CuimZnL_{-2H})(CuimZnL_{-H})](ClO_4)_3$ (2). The ESR spectra of complex **2** in frozen 50% aqueous DMSO solution at 110 K as a function of pH are shown in Figure 9. The spectra of the complex, in the range 6.2 ≤ pH ≤ 9.5, exhibit the signals for the Cu−im−Zn species, since the parameters are the same as those of the original complex **2** as already mentioned (Figure 5b), indicating that the Cu−im−Zn species as the majority is still retained in these solutions in this pH range. Another set of parameters is obtained for two curves at pH 10.6 and 11.7 ($g_{\|} = 2.00$, $g_{\perp} = 2.23$, $A_{\|} = 81.7$ G, and $A_{\perp} = -101$ G), suggesting the formation of another Cu(II) species in trigonal pyramidal geometry. When the pH is lower than 4.0, the signals of free Cu(II) ions appeared, suggesting the damage of the imidazolate bridge, and then, the bridged structure dissociated completely at pH = 2.7, which is similar to the behavior of complex **1**.

To elucidate the details of the solution behavior for complex **2**, the pH-dependent UV−vis spectrometry for **2** in water solution was recorded in the range 2.00 ≤ pH ≤ 11.96 (Figure 10). The spectra were found to be almost unchanged in the range 5.85 ≤ pH ≤ 9.91 and were similar to that of **2** dissolved directly in aqueous solution. Below pH = 5.85, the visible spectrum was markedly changed, indicating the breakage of the imidazolate bridge. Above pH 9.91, the visible spectrum was also evidently changed, and more than one isosbestic point was observed, suggesting more complex behavior.

These results demonstrate that the imidazolate-bridged Cu−im−Zn moieties of complex **2** in aqueous solution can be stable over a pH range ca. 6−10 in solution. The solution behavior above pH 10 is more complicated than that of **1**.

(36) Koike, T.; Kajitani, S.; Nakamura, I.; Kimura, E.; Shiro, M. *J. Am. Chem. Soc.* **1995**, *117*, 1210.

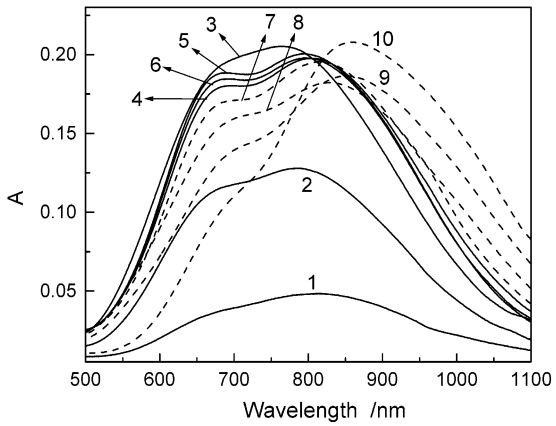

Figure 10. electronic spectra of **2** in aqueous solution recorded as a function of pH. From 1 to 6 for solid lines: pH = 2.00, 3.10, 5.70, 5.85, 7.44, and 8.54. From 7 to 10 for dashed lines: pH = 9.91, 10.04, 10.97, and 11.96.

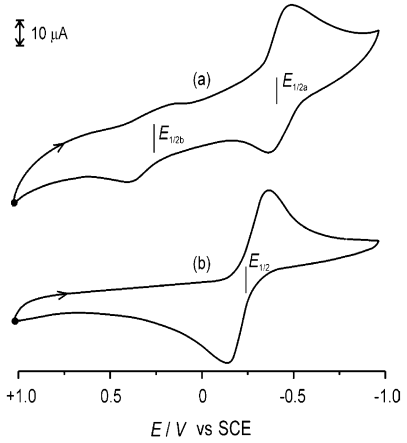

Figure 11. Cyclic voltammograms of (a) $[(CuimCu)L](ClO_4)_3 \cdot 0.5H_2O$ (**1**, 1.0 mM) and (b) $[(CuimZnL_{-2H})(CuimZnL_{-H})](ClO_4)_3$ (**2**, 0.5 mM) in DMF containing 0.1 M TBAP: working electrode, glassy carbon; counter electrode, Pt wire; reference electrode, saturated calomel electrode; scan rate, 50 mV s^{-1}.

Electrochemistry. The electrochemical properties of the two complexes have been studied by cyclic voltammetry (CV) in degassed DMF solution. Figure 11 shows the cyclic voltammograms of complexes **1** and **2**. The CV of complex **1** shows two quasireversible redox waves at $E_{1/2a} = -0.39$ V and $E_{1/2b} = +0.25$ V (vs SCE), corresponding to the Cu(II,I)/Cu(I,I) and Cu(II,II)/Cu(II,I) redox couples, respectively.[18b] The CV of complex **2** exhibits only one reversible Cu(II)/Cu(I) redox couple at $E_{1/2} = -0.25$ V (vs SCE), which indicates that there is only one copper ion in the complex. The difference in Cu(II)/Cu(I) redox potential between complexes **1** and **2** demonstrates that the coordination environments around the copper(II) ions of the two complexes are different and afford a substantial explanation for the difference in SOD activity of them (see the following subsection). It is known that an adequate Cu(II)/Cu(I) redox potential for effective catalysis of superoxide radical must be required between $E^\circ = -0.16$ V versus NHE (−0.405 V vs SCE) for O_2/O_2^- and $E^\circ = 0.89$ V versus NHE (0.645 mV vs SCE) for O_2^-/H_2O_2. Though it is inappropriate to compare the $E_{1/2}$ values with the reduction potentials of the couples O_2/O_2^- and O_2^-/H_2O_2, the redox potential of the two complexes in DMF should be in the allowed ranges of an SOD mimic, since the obtained results of SOD activity assay showed that both of them have relatively high activity.

Table 4. SOD Activities (IC_{50} Values) of Model Complexes and Native Cu_2,Zn_2-SOD

complexes	IC_{50}[a] (μM)	ref
1	0.62	this work
2	0.26	this work
$[Cu(im)ZnL']^{3+}$	0.50	18a
$[Cu_2(bdpi)(CH_3CN)_2]^{3+}$ [b]	0.32	18b
$[Cu_2(Me_4bdpi)(H_2O)_2]^{3+}$	1.1	18b
$[CuZn(Me_4bdpi)(H_2O)_2]^{3+}$ [c]	0.24	18b
$[Cu_2(bpzbiap)Cl_3]$[d]	0.52	17
native Cu_2,Zn_2-SOD	0.04	7

[a] The IC_{50} value is for one Cu(II) ion. [b] bdpi = 4,5-bis(di(2-pyridylmethyl)aminomethyl)imidazolate. [c] Me_4bdpi = 4,5-bis(di(6-methyl-2-pyridylmethyl)aminomethyl)imidazolate. [d] Hbpzbiap = 1,5-bis(1-pyrazolyl)-3-[bis(2-imidazolyl)methyl]azapentane.

Superoxide Dismutase Activities. The SOD-like activities of the two complexes were investigated by NBT assay, and catalytic activity toward the dismutation of superoxide anion was measured. The macrocycle with two hydroxyethyl arms provides a stable and flexible environment similar to that in the active site of the native enzyme, ensuring the stable existence of the complexes at the investigated pH value in aqueous solution. In this work, the SOD-like activities for the two complexes were measured at pH = 7.8, and the already discussed pH-dependent ESR study has clearly revealed that the imidazolate-bridged Cu(II)−Cu(II)/Cu(II)−Zn(II) components are stable in aqueous solution at pH = 7.8; thus, the measured SOD-like activity should be attributed to the two complexes themselves.

The chromophore concentration required to yield 50% inhibition of the reduction of NBT (IC_{50}) was determined by following the literature method.[26] The IC_{50} values are listed in Table 4, together with the values of the best SOD models so far reported. The IC_{50} values of for complexes **1** and **2** are 0.62 and 0.26 μM, respectively. They are among the most active model compounds but are somewhat less active than the native enzyme ($IC_{50} = 0.04$ μM).

The difference in IC_{50} values for the two complexes should be ascribed to the evident discrepancy in the structures between them, especially in the conformation of the ligand. The good activities of the two complexes may be attributed to the flexible macrocyclic ligand, which is able to accommodate the geometrical change from Cu(II) to Cu(I),[18a] especially the two labile hydroxyethyl arms, which are proposed to be easily substituted by the substrate, O_2^-, in the catalytic process, just like the O_2^- in place of the water molecule bound to the copper site in the mechanism of dismutation of superoxide anion by native SOD.

Conclusion

In this paper, we reported the syntheses, structures, and properties of two imidazolate-bridged bimetallic complexes, $[(CuimCu)L]ClO_4 \cdot 0.5H_2O$ (**1**) and $[(CuimZnL_{-2H})(CuimZnL_{-H})](ClO_4)_3$ (**2**), of a new single macrocyclic ligand

with two hydroxyethyl pendants. The imidazolate bridges in the two complexes have been found to be stable over broad pH ranges, 5−12 for **1** and 6−10 for **2**, respectively. The SOD-like activity evaluation reveals that the complexes are among the list of the models with the highest activity, and the labile hydroxyethyl pendants are believed to play an important role in the catalytic process.

Generally, it is difficult to obtain heterodinuclear complexes with a symmetric binucleating ligand. This work may provide a new technique for holding different metal ions in close proximity which involves placing them within the confines of a flexible single macrocyclic ring.

Acknowledgment. This work is supported by the National Natural Science Foundation of China.

Supporting Information Available: X-ray crystallographic data in CIF format. This material is available free of charge via the Internet at http://pubs.acs.org.

IC034338G